

Sparse Signal Reconstruction with QUBO Formulation in l_0 -regularized Linear Regression

Naoki Ide

Advanced Research Laboratory, R&D Center, Sony Corporation
Tokyo, Japan
Naoki.Ide@sony.com

Masayuki Ohzeki

Sigma-i Co., Ltd, Tohoku University, Tokyo Tech
Tokyo, Japan
mohzeki@sigmailab.com

Abstract— An l_0 -regularized linear regression for a sparse signal reconstruction is implemented based on the quadratic unconstrained binary optimization (QUBO) formulation. In this method, the signal values are quantized and expressed as bit sequences. By transforming l_0 -norm to a quadratic form of these bits, the fully quadratic objective function is provided and optimized by the solver specialized for QUBO, such as the quantum annealer. Numerical experiments with a commercial quantum annealer show that the proposed method performs slightly better than conventional methods based on orthogonal matching pursuit (OMP) and the least absolute shrinkage and selection operator (LASSO) under several limited conditions.

Keywords—sparse, signal reconstruction, l_0 -norm QUBO, quantum annealing

I. INTRODUCTION

Sparse signal reconstruction is a technique that recovers an original representation from relatively few observed signals. Although this problem is usually ill-posed for linear systems, there are several algorithms that perfectly recover the original representation with sufficient sparsity [1,2].

Direction-of-arrival (DOA) estimation in array signal processing is one of the applications of the sparse signal reconstruction. In this application, the directions of the signal sources such as sound sources and radar targets be estimated through the use of the sparse signal reconstruction schemes[3]. Since the signal sources usually appear sparsely along the azimuth axis, the distribution of these sources can be estimated through the use of such schemes.

In these sparse signal reconstruction techniques, the algorithms are usually based on l_1 -regularized linear regression (LASSO) [1] which is an unconstrained extension of l_1 -norm minimization that minimizes the l_1 -norm, the sum of absolute values of the representation vector. When the order of the regularization is generalized as p , the objective function of l_p -regularized linear regression is described as,

$$L_p(z) = \frac{1}{2\gamma_p} \|x - Az\|_2^2 + \|z\|_p, \quad (1)$$

where $z \in \mathbb{C}^M$ is a vector for a sparse representation, $x \in \mathbb{C}^N$ is a vector for observed signals, $A \in \mathbb{C}^{N \times M}$ with ($N < M$) is an observation matrix, γ_p is a regularization parameter and $\|z\|_p$ represents p -norm of z . For $p = 1$, an l_1 -norm is to be minimized.

In l_0 -norm minimization, which is for $p=0$, an l_0 -norm, the number of nonzero entries in sparse signal, is concern. Several theoretical considerations indicate that the l_0 -norm minimizations are in principle superior to the l_1 -norm minimizations [4]. However the implementation is practically difficult due to the potential threat of the combinatorial

explosion, which forces us to use approximate approaches based on greedy policy, such as orthogonal matching pursuit (OMP) [5].

Quantum annealing [6] is a method that can tackle such laborious computations. This method efficiently solves a certain type of optimization problems using a QUBO formulation. The objective function of the QUBO is expressed as a quadratic form of n binary variables:

$$L(b) = b^T Q b, \quad (2)$$

where $b \in \{0,1\}^n$ is a vector of binary variables, and $Q \in \mathbb{R}^{n \times n}$ is a matrix of quadratic coefficients.

In this paper, we propose a method for the sparse signal reconstruction that solves the l_0 -regularized linear regressions with quantum annealing. In the following sections, we explain the QUBO-based technique, and compare the performance of the proposed method with that of the conventional methods.

II. SPARSE SIGNAL RECONSTRUCTION

A. Conventional techniques

To solve a QUBO problem by quantum annealing, the binary variables need to be expressed as variables $s \in \{-1,1\}^n$. When $b = (1 - s)/2$ is substituted into (2), the objective function for the quantum annealing is expressed as

$$H(s) = - \sum_{i=1}^n \sum_{j<i}^n J_{ij} s_i s_j - \sum_{k=1}^n h_k s_k, \quad (3)$$

where $J \in \mathbb{R}^{n \times n}$ and $h \in \mathbb{R}^n$ are the coefficient matrices. When the coefficients $\{J, h\}$ in $H(s)$ are given to the quantum annealer the solution s^* is provided from it and the solution b^* is obtained by $b^* = (1 - s^*)/2$.

The function $H(s)$ is the energy function for the spin system in the Ising model. Thus, $H(s)$ is minimized, when the Ising spin system is achieving the ground state of the model. To achieve this ground state effectively, the quantum annealer uses an annealing process that controls quantum fluctuation appropriately to explore the solution space. This annealing process is performed in the discrete time steps. In each step, sufficient time is given in order for the system to converge to the ground state of the following Hamiltonian:

$$H_t(\sigma) = (1 - \Gamma_t) H_p(\sigma^z) - \Gamma_t \sum_{k=1}^n \sigma_k^x, \quad (4)$$

where σ is the Pauli spin operators for n spins, and σ^z, σ^x are z and x elements of σ , respectively. In (4), the second term represents quantum fluctuation, and Γ_t is a parameter that controls the balance between two terms at step t . While the first term provides the system with the convergence to the

ground state (QUBO solution), the second term provides the system with the superposition of all possible vectors to explore the solution space. Typically, Γ_t starts from 1 for the initial superposition, and it gradually decreases to 0 to converge the system to the ground state. At the last step, the annealer provides a solution s^* as the measurement value of σ^z .

The mechanism of quantum annealing is similar to simulated annealing, which numerically simulates thermal fluctuation. However, their performances are different because the quantum fluctuation generating tunneling effect, which enables state transition over a relatively large energy barrier in (3). Theoretical analysis has proved the superiority of the quantum annealing on the computation time over the simulated annealing [7]. However, the prove was not the theoretical guarantees for drastic acceleration of computation time like factorization in quantum gate computing.

The quantum annealing hardware system produced by D-Wave Systems [8] performs quantum annealing at the device level. In this system, the variables s and the coefficients $\{J, h\}$ are embedded on the qubit devices and their hardware parameters, respectively. The number of the available qubits (spins) has been growing in scale since 2011, and currently is approximately 5000. In the implementation of the Ising spin system, the physical network of qubits devices is automatically generated with the program coded using the dedicated software libraries. In addition, there is also software tool for extracting the input parameters $\{J, h\}$ from the program codes about the objective function instead of an explicit expression of Q [9]. Therefore, research topics on quantum annealing have spread to QUBO formulation methods for various combinatorial optimization problems. For example, the Karp's NP-complete problems are formulated as QUBO in [10]. Several studies on robotics and wireless communications [11,12] have provided QUBO's formulation for the methods that were hampered by combinatorial explosions, demonstrated the possibility of a solution using quantum annealing.

In [13,14], binary compressed sensing is formulated by QUBO and implemented using the quantum annealer. Binarizing the representation is a simple approach to linearizing the nonlinear regularization term. However, this approach can result in inadequate resolution. Also, since there is no difference between l_1 -norm and l_0 -norm, it is uncertain whether the benefits of l_0 -norm minimization will be obtained. To avoid this problem, the multi-level quantization for the representations is used in the proposed method.

B. Proposed technique

We propose a K -bit-quantized technique ($K > 1$), which decomposes a representation vector $z \in \mathbb{R}^M$ as

$$z = Bw, \quad (5)$$

where $B \in \{0,1\}^{M \times K}$ is a matrix of binary variables to be optimized, and $w \in \mathbb{R}^K$ is a weight vector. If $w_k (k = 1 \dots K)$ is 2^{-k} , the quantization covers the representation value in range $[0,1]$ with 2^K grids. If w_1 is -2^{-1} , the covering range moves to $[-0.5, 0.5]$ and both positive and negative values are available. This quantization provides the following expression of the objective function for the l_0 -regularized linear regression:

$$L(B) = \frac{1}{2\gamma_0} \|x - ABw\|_2^2 + \|Bw\|_0, \quad (6)$$

where γ_0 is a regularization coefficient.

To utilize the quantum annealing processing, each term of (6) has to be quadratic. While the first term is obviously quadratic, the second term is not apparent. To express the second term in a quadratic form, we formulate this with binary variables, and transform it into the quadratic form.

Since the product of the inversed bits is 0 for nonzero number and 1 for zero in binary expression, the l_0 -norm (number of nonzero elements) in (6) is expressed as:

$$\|Bw\|_0 = \sum_{i=1}^M \left(1 - \prod_{k=1}^K (1 - b_{ik}) \right), \quad (7)$$

where b_{ik} is the k -th bit for the i -th representation entry. The value inside the large parenthesis takes 1 if any of $b_{ik} (k = 1 \dots K)$ takes 1, which means z_i is nonzero.

Although (7) is a binary form, it is not quadratic for $2 < K$ and needed to reduce the dimension. For this reduction, it is effective to replace product of two binary variables with another binary variable, as the product also takes only 0 or 1. To reduce the dimension of (7), the product in (7) is replaced with auxiliary variables $C \in \{0,1\}^{M \times (K-2)}$ as following way:

$$\begin{aligned} \prod_{k=1}^K (1 - b_{ik}) &= c_{i1}(1 - b_{i3}) \dots (1 - b_{iK}) \\ &= c_{iK-2}(1 - b_{iK}), \end{aligned} \quad (8)$$

where $c_{ik} (k = 1 \dots K - 2)$ is i, k element of C .

Although (8) is quadratic, the optimization of (8) is different from QUBO, as it requires the following constraints for the variables c_{ik-1}, c_{ik} , and b_{ik+1} ,

$$c_{ik} = c_{ik-1}(1 - b_{ik+1}), \forall k = 1, 2, \dots, K - 2, \quad (9)$$

with $c_{i0} = 1 - b_{i1}$.

To make this an unconstrained optimization, we add a penalty term, which takes 0 only when the constraints are satisfied otherwise takes a positive value. When we consider a relation $c = ab$ for the binary variables a, b , and c , one possible scheme that provides appropriate penalty is $(c - ab)^2 = c + ab - 2abc$. However, it still contains a triple factor term, abc . To remove abc , we further add $2(1 - a)(1 - b)c$, which also takes 0 when $c = ab$. Then, the final penalty term is

$$p(a, b, c) = 3c + ab - 2ac - 2bc, \quad (10)$$

With Equation (8), (10) and a positive real parameter λ_c , the objective function is now described:

$$\begin{aligned} L_p(B, C) &= \frac{1}{2\gamma_0} \|x - ABw\|_2^2 \\ &+ \sum_{i=1}^M \left(1 - c_{iK-2}(1 - b_{iK}) \right. \\ &\left. + \sum_{k=1}^{K-2} \lambda_c p(1 - b_{ik+1}, c_{ik-1}, c_{ik}) \right). \end{aligned} \quad (11)$$

The objective function obtained here becomes fully quadratic in terms of B and C . With the parameters $\{J, h\}$ available from the observations, (11) can be evaluated using the quantum annealer.

C. Extension for multiple observation

In this setting, the reconstruction system is assumed to use the multiple observations of the different representations generated from the original representation. In the generating process for the representations, the nonzero entries in the original representation variate stochastically.

The l_1 -SVD (singular value decomposition) [3] is a method that handles the observations by group l_1 -regularized linear regression (group LASSO). When the S observations are obtained as $X = (x_1 \dots x_S) \in \mathbb{C}^{N \times S}$, the objective function of group-LASSO is expressed as:

$$L(Z) = \frac{1}{2\gamma_1} \|X - AZ\|_2^2 + \|l_2(Z)\|_1, \quad (12)$$

where $Z = (z_1 \dots z_S) \in \mathbb{C}^{M \times S}$ is a representation matrix, and $l_2(Z)$ is a set of l_2 norms for Z along the axis for S .

In addition, this method reduces the computational costs with an SVD-based preprocess. This process provides the optimizer with $X_L = (u_1 \dots u_L) \in \mathbb{C}^{N \times L}$ from the decomposed form $X = U\Sigma V$ instead of X . This substitution causes difference between the representations with and without the preprocess. However the entries that takes 0 in the original representation are assured to take 0.

To accommodate the scenario for the multiple observation scenario, we modify (5) to the following form:

$$Z = Bw, \quad (13)$$

where $B \in \{0,1\}^{M \times L \times K}$ is the $M \times L \times K$ tensor with binary variables to be optimized, L is the number of observations and $w \in \mathbb{R}^K$ is the weight vector as same in (5). The matrix $Z \in \mathbb{C}^{M \times L}$ consists of the representations $z_1, z_2 \dots z_L \in \mathbb{C}^M$ whose nonzero positions are also the nonzero position in the original representation $\zeta \in \mathbb{C}^M$. From this regulation, the number of the nonzero in ζ is inferred greater or equal to the number of the nonzero rows in Z , which allows approximation of $\|\zeta\|_0$ with $\|l_2(Z)\|_0$. Thus, the objective function is expressed as

$$L(B) = \frac{1}{2\gamma_0} \|X - ABw\|_2^2 + \|l_2(Bw)\|_0. \quad (14)$$

Similar to (8), the l_0 -norm group can be obtained as:

$$\|l_2(Z)\|_0 = \sum_{i=1}^M \left(1 - \prod_{l=1}^L (1 - c_{iik-1}) \right), \quad (15)$$

where $C \in \{0,1\}^{M \times L \times (K-1)}$ is the auxiliary binary variables. Similar to the derivation for (11), we obtain the objective function of the l_0 -norm-group-regularized linear regression as

$$\begin{aligned} L_p(B, C, D) = & \frac{1}{2\gamma_0} \|X - ABw\|_2^2 \\ & + \sum_{i=1}^M \left(1 - d_{iL-1} \right. \\ & + \sum_{l=1}^{L-1} \left(\lambda_c p(1 - c_{iik-1}, d_{iL-1}, d_{il}) \right. \\ & \left. \left. + \sum_{k=1}^{l-1} \lambda_d p(1 - b_{iik+1}, c_{iik-1}, c_{iik}) \right) \right), \end{aligned} \quad (16)$$

where $D \in \{0,1\}^{M \times (L-2)}$, and λ_d is a positive real parameter.

This objective function has the quadratic and linear terms, which consist of the binary variables, B , C and D . To evaluate this equation, we extract parameters $\{J, h\}$ from the observations X and reconstruct Z from obtained B with (13).

The l_0 -SVD is obtained as an extension of the optimization for (16) with the SVD preprocess in the l_1 -SVD.

III. EXPERIMENT

A. Setup

All the quantum annealing process was performed on D-Wave Advantage Systems 4.1. The program codes for the proposed method were executed remotely through the cloud interface. We used a Python library, dwave-ocean-sdk 3.1.0, installed on a Windows 10 machine with an Intel Core i7-CPU and 64 GB of RAM. For the comparison of these results, simulated annealing computation was performed using dwave-neal as a reference for the same QUBO problems. We also used pyqubo 1.0.0 to extract $\{J, h\}$ from the program codes. For LASSO, OMP, SVD, and group-LASSO, we utilized publicly available libraries, including sklearn, numpy, and group-lasso.

In the evaluation, the original sparse representations were sampled with random values for randomly selected nonzero entries. The observations were simulated with the sampled representations and given observation matrices explained later. The proposed and the reference methods reconstructed the original sparse representations from the given observation, and the accuracy on the nonzero elements detection was evaluated for each method. Specifically, the method that provided the reconstruction whose nonzero positions matches exactly for the original representations were given the score 1, and 0 otherwise. We repeated the evaluation procedure typically 100 times and used the average score as reconstruction success rates. In addition, we monitored the achieved values of (6) for the original representation z , quantized representation q , and reconstructed representation s and those of (11) for s .

In the DOA estimation, since the observation matrix $A \in \mathbb{C}^{N \times M}$ is composed of the steering vectors, a_{nm} , the complex-valued elements at (n, m) is expressed as

$$a_{nm} = \exp \left(2\pi i \frac{nd}{\lambda} \sin \left(2\pi \left(\frac{m}{M} - \frac{1}{2} \right) \right) \right), \quad (17)$$

where n represents the n -th sensor of the sensor array, m represents the m -th azimuth grid, λ is the wavelength of the signal carrier and d is the distance of each array elements, typically, $d = 0.5\lambda$ is chosen.

Here, we modify the observation matrix by replacing $\pi(2m/M - 1)$ with $\arcsin(2m/M - 1)$ and obtain

$$a_{nm} = (-1)^n \exp \left(2n\pi i \frac{m}{M} \right). \quad (18)$$

This expression is similar to the top N rows of the $M \times M$ discrete Fourier transformation, except that its sign depends on row indices. Although this grid arrangement becomes non-uniform, the similarity to the discrete Fourier transformation is useful. In addition, with this configuration, (18) provides a higher resolution than in (17) in the middle of the azimuth angles. For instance, when $M = 160$, it is calculated that the resolution inside angle $\pm 45^\circ$ becomes less than 1° , which is finer than in the uniform spacing.

B. Results for Single Observation

We observed the experimental results for the observation matrix in (18) with representation sizes of $M = 32, 64, 128, 256$ and 512 and observation densities of $N/M = 1/8, 1/4, 3/8$ and $1/2$. For each settings, the original representations were sampled under 9 or 10 different sparsity (nonzero density) conditions. The range of the representation values was set for $[0, 1]$. For the proposed method, we set $K = 4$ for the bit length of quantization, $\gamma_0 = 0.5^{10} \sim 0.001$ for the l_0 -regularization parameter supposed to be 0.5^d ($d = 0, 1 \dots$) and $\lambda_c = 1.5$ for penalty parameter supposed to be $0.5d$ ($d = 0, 1 \dots$). As the reference methods, we used LASSO and OMP from sklearn.

Fig. 1 shows the reconstruction success rates (left) and the achieved values (right) for the representation size of $M=32$ and the observation density of $N/M=1/4$. For LASSO, we set $\gamma_1 = 0.5^{11} \sim 0.0005$ supposed to be 0.5^d ($d = 0, 1 \dots$) as the best values for $M = 32$. In the evaluation, the threshold 0.02 is set to avoid false positive detection in the reference methods. In the left graph, the proposed method performed clearly higher scores than the other methods except for left 2 plots. This was observed for $N/M = 1/8$ and $3/8$, but not for $N/M = 1/2$ and $M > 64$. The reconstruction errors in the left 2 plot were observed mainly false-negative in the nonzero detection. The right graph shows that the value of (6) for the recovered representation ($L(s)$) did not achieve those of the original representation ($L(z)$). From the comparison of $L(s)$ with the values of (6) for the quantized representations ($L(q)$), the quantization error was dominant for the difference between $L(s)$ and $L(z)$ in left 4 plots. Also from the comparison of $L(s)$ with the achieved values of (11) ($L_p(s)$), the penalties in (11) were 0, indicating that the constraint in (9) were satisfied.

Fig. 2 shows the results for $M=32$ and $N/M=1/4$ with 8-bit resolution ($K=8$). The left graph shows deterioration due to the large K in the proposed method. This deterioration was observed gradually increasing when K was greater than 4. The right graph shows the increase in $L(s)$ and decrease in $L(q)$ for the increased K . The increase of the difference between $L(s)$ and $L(q)$ indicates the optimization became insufficient.

Fig. 3 shows the results for $M=512$ and $N/M=1/4$ with 4-bit resolution ($K=4$). We set $\gamma_1 = 0.5^{14} \sim 0.0005$ for LASSO as the best values for $M = 512$. In the left graph, the proposed method did not performed better than the reference method. However, the deterioration from the large M was smaller than that from the large K . The right graph shows that the difference between $L(s)$ and $L(q)$ increased for the increased M , which indicates that the optimization became insufficient, but the increase of the difference was not as large as in Fig.2. Instead of the deterioration from the quantization error becomes larger from the comparison of $L(q)$ and $L(z)$.

Fig. 4 shows the result for $M=512$, $N/M=1/4$ and $K=4$. In this experiment, Gaussian noise with standard deviation 0.01 were added to each observations. We set $\gamma_1 = 0.5^{14} \sim 0.0005$ for LASSO and we used the threshold value $0.5^4 \sim 0.02$ to avoid the erroneous nonzero detection. The left graph shows deterioration in both the proposed method and the reference methods compared with Fig.3. However the degree of deterioration was less in the proposed method than the others. The right graph shows that the increase in $L(q)$ and $L(z)$ due to the observation noise. However, the increase in $L(q)$ is not observed in $L(s)$ except for the left 3 plots, indicating that the proposed method was robust to the observation noise. These

tendency were observed for other observation densities. We all observed the results for the other representation size with the observation noise (std = 0.01). The proposed method performed better than the reference methods also for $M=64$, which indicates that the proposed method is relatively robust for the observation noise.

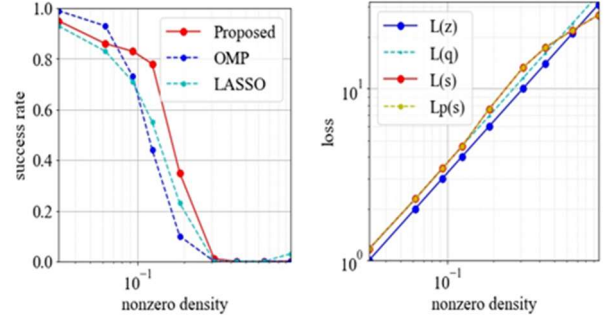


Fig. 1. Success rate of reconstruction (left) and loss values (right). The x -axis represents the density of nonzero representations. We evaluated 100 samples with a 32-dim representation and 8-dim observation with 4-bit quantization. Representation values are limited to $[0, 1]$.

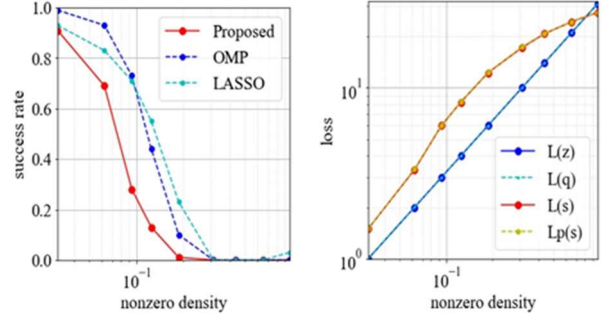


Fig. 2. Success rate (left) and loss values (right) for higher resolution. We sampled 100 problems with an 8-dim observation and 32-dim representation and evaluated our method with 8-bit quantization.

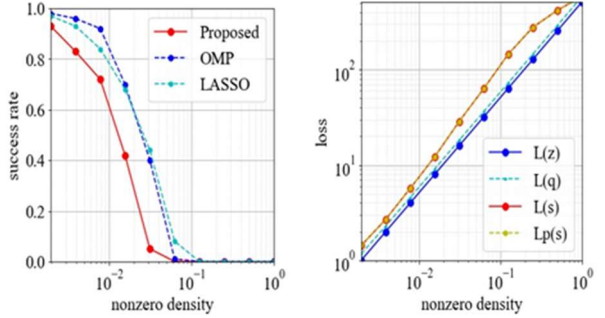


Fig. 3. Success rate (left) and loss values (right). We evaluated 100 samples with a 512-dim representation and 128-dim observation. We used our method with 4-bit quantization.

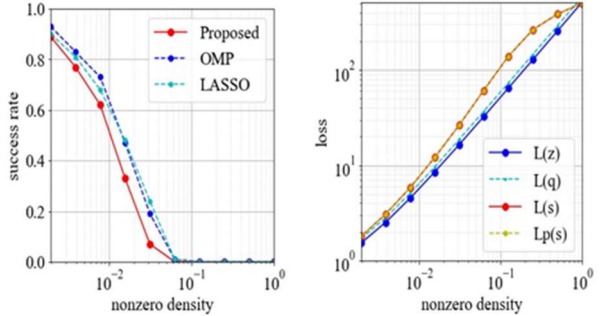


Fig. 4. Success rate (left) and loss values (right). We added white Gaussian noise (std: 0.01) for noisy observations. We evaluated 100 samples with a 512-dim representation and 128-dim observation. We used our method with 4-bit quantization.

C. Results for Multiple Observations

We also conducted experiments to compare the proposed l_0 -SVD with the conventional l_1 -SVD. For the multiple observation setting, S representations are sampled to generate X with the matrix A given in (18). To generate the representations Z , we duplicate the original representation ζ S times adding random values for each. We set the random value as normal distributed random value with amplitude of $\rho\zeta$ ($\rho > 0$), which provides the fluctuation only for the nonzero elements of ζ . The SVD preprocess provides with the proposed method and the reference methods with the left L block of U in the decomposed form $X = U\Sigma V^T$. In this setting, both the proposed l_0 -SVD and the conventional l_1 -SVD are provided the L observations X_L to reconstruct L representations. In the evaluation phase, the first representation among L was used.

We observed the experimental results with representation sizes for $M = 64$ and 160 , the observation densities for $N/M = 1/8, 1/4, 3/8$ and $1/2$, the number of observation shot for $S=16$, the range of values in the original representation ζ for $[0,1]$ and fluctuation coefficients for $\rho=0.1$. For the proposed method, we set the bit length for $K = 4$, the regularization coefficient for $\gamma_0 = 0.5^{11} \sim 0.001$, the penalty coefficients for $\lambda_c = \lambda_d = 1.5$. As reference methods, we prepared the l_1 -SVD and an extension of LASSO, which uses the average vector of $S=16$ observations. The regularization coefficients of both l_1 -SVD and LASSO is set to $\gamma_1 = 0.5^{14} \sim 0.0005$. The number of the observations after SVD preprocess is set to $L=2$ for both l_0 -SVD and l_1 -SVD.

Fig. 5 shows the result for $M=160, N/M = 1/4$ and $K = 4$. The left and right graphs show the results for the clean ($\sigma=0$) and the noisy ($\sigma=0.05$) observations, respectively. In both the left and right graphs, the proposed method did not show advantage over the reference methods. In addition, the proposed method were not robust than the conventional methods in this settings. The similar tendency was observed in the different observation densities. We also observed the results for $M=64$, the difference between the proposed and the reference methods was smaller than the results for $M=160$.

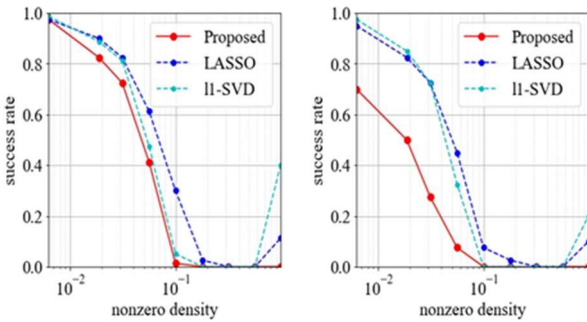


Fig. 5. Success rate for the clean (left) and the noisy (right) observations. We evaluated 50 samples of 16 shots, 40-dim observations generated from 160-dim representations. In the right graph, we added Gaussian noise (std: 0.05) for the observations.

IV. DISCUSSION

The proposed method performed slightly better than the conventional methods for the small and coarse representations and the noisy observations but did not for other conditions including multiple observation setting. In the following, we discuss the mechanism of the better performance and the cause of the performance deterioration.

A. Effect of Quantization

We consider the better performance is caused by the compensation effect from the discretization of the solution space.

As in the experiment section, it is useful to analyze the achieved values $L(s), L(z)$ and $\delta = L(s) - L(z)$ where L is the objective function in (1), and z, s are the original and recovered representation, respectively. With this value, the success in the exact recovery is ensured by $\delta > 0, (\forall s \neq z)$. When the observation with noise n to be $x = Az + n$, δ is expressed as:

$$\delta = \frac{1}{2\gamma_p} \|Ae\|_2^2 + (\|e + z\|_p - \|z\|_p) - \frac{1}{\gamma_p} e^T An, \quad (19)$$

where $e = s - z \neq 0$. The criteria is applicable for the quantized form of z , by adding the quantization error r to the noise n via $n + Ar$.

To achieve better performance, the greater bias (the first and second terms) and less variance (the third term) is needed in (19). Although the variance in δ increases due to the quantization, the bias in δ takes discretized values that provides margin to hold the optimum of δ against perturbation. Intuitively, this margin is wider in the coarser representation, the proposed method shows the robustness. To confirm this quantitatively, we will numerically estimate the degree of this effect in future work.

B. Dependency on the problem size

As shown in the graphs for the achieved values, we observed that optimizations did not reach the minimum for the larger representations and the finer quantization. It is assured theoretically that quantum annealing provides the global optimum in high probability with sufficient annealing time [7]. However the current quantum annealer has several issues that prevent achieving the ideal optimization.

The insufficient annealing time is one of the issues mainly from the collapse of quantum states (coherence time) due to environmental disturbance. Theoretically, the required time increases by exponential order for number of qubits, it is essential to reduce the number of the binary variables. In case of the proposed method, it requires MKL bits for B , $ML(K - 1)$ bits for C and ML bits for D in (16).

Another issue is the insufficient resolution that causes by embedding the coefficients $\{J, h\}$ on analog values of the hardware. From the first term of (16), the required resolution is roughly estimated as $2^{-K}\gamma_0$ when γ_0 takes sufficiently small value. It is obvious that the more resolution is required in the larger K and also when the parameter γ_0 is required to be smaller.

V. CONCLUSION

An l_0 -regularized linear regression based on the QUBO formulation was evaluated its performance on the sparse signal reconstruction with the aid of the commercial quantum annealer. The proposed method performed slightly better than the conventional methods under several limited conditions. The analysis showed the mechanism of the advantage and the cause of the insufficient optimizations. These results indicate the potential of the better performance in the proposed method by the improvement of the quantum annealer and the recent QUBO solvers

REFERENCES

- [1] R. Tibshirani, "Regression Shrinkage and Selection via the Lasso," *J. R. Stat. Soc. Series B*, vol. 58, pp. 267–288, 1996.
- [2] D. L. Donoho, "Compressed sensing," *IEEE Trans. Inf. Theory*, vol. 52, pp. 1289–1306, April, 2006.
- [3] D. Malioutov, M. Cetin, and A. S. Willsky, "A sparse signal reconstruction perspective for source localization with sensor arrays," *IEEE Trans. Signal Process.*, vol. 53, pp. 3010–3022, August. 2005.
- [4] E. J. Candès, "The restricted isometry property and its implications for compressed sensing," *C. R. Math.*, vol. 346, pp. 589–592, May. 2008.
- [5] G. Mallat and Z. Zhang, "Matching pursuits with time-frequency dictionaries," *IEEE Trans. Signal Process.*, vol. 41, pp. 3397–3415, December. 1993.
- [6] T. Kadowaki and H. Nishimori, "Quantum Annealing in the Transverse Ising Model," *Phys. Rev. E*, vol. 58, pp. 5355–5363, November. 1998.
- [7] S. Morita and H. Nishimori, "Mathematical foundation of quantum annealing," *J. Math. Phys.*, vol. 49, 125210, 2008.
- [8] M. W. Johnson et al., "Quantum annealing with manufactured spins," *Nature*, vol. 473, pp. 194–198, May. 2011.
- [9] <https://pyqubo.readthedocs.io/en/latest/>
- [10] A. Lucas, "Ising formulations of many NP problems," *Front. Phys.*, vol. 2, a5, February. 2014.
- [11] M. Ohzeki, A. Miki, M. J. Miyama, and M. Terabe, "Control of automated guided vehicles without collision by quantum annealer and digital devices," *Front. Comput. Sci.* 1-9 November 2019.
- [12] N. Ide, T. Asayama, H. Ueno, and M. Ohzeki, "Maximum Likelihood Channel Decoding with Quantum Annealing Machine," *Proc. 2020 Int. Symp. Inf. Theory Appl., ISITA 2020*, pp. 91–95, 2020.
- [13] R. Ayanzadeh, S. Mousavi, M. Halem, and T. Finin, "Quantum annealing based binary compressive sensing with matrix uncertainty," <https://arxiv.org/abs/1901.00088>.
- [14] R. Ayanzadeh, H. Milton, and T. Finin, "An ensemble approach for compressive sensing with quantum annealers," *IEEE International Geoscience and Remote Sensing Symposium*, pp. 3517–3520R, 2020.
- [15] H. Friedman and J. Tibshirani, "Regularization Path for Generalized Linear Models by Coordinate Descent," *J. Stat. Softw.*, vol. 33, pp. 1–22, February. 2010.
- [16] R. Zibulevsky and M. Elad, Efficient Implementation of the K-SVD Algorithm using Batch Orthogonal Matching Pursuit Technical Report, CS Technion, April. 2008.